THE ELUSIVE DUST TORUS UNVEILED BY ADAPTIVE OPTIC OBSERVATIONS FROM 2.2 μm TO 4.8 μm

D. ALLOIN
Service d'Astrophysique, CE Saclay, France

AND

O. MARCO
DESPA, Observatoire de Paris, France

Abstract.

Adaptive optic systems allow to probe in the near-infrared the inner structure of AGN at a resolution close to that achieved with the Hubble Space Telescope at visible and ultraviolet wavelengths.

The nuclear region of NGC 1068 has been mapped in the near-infrared at 2.2, 3.5 and 4.8 μm, with the ESO adaptive optic system.

These data show the presence of strong near-infrared emission within the central 100 pc around the nucleus. For both K, L and M bands, the dominant emission peak is unresolved at resolutions of respectively 35 pc (K), 15 pc (L) and 23 pc (M).

The emission peaks at 2.2, 3.5 and 4.8 μm are found to be offset by 0.3$\pm$0.1" south of the HST optical continuum peak. The infrared peaks are coincident with the HST imaging polarimetry center thought to trace the hidden nucleus.

We conclude that the infrared emission peaks are also directly related with the hidden nucleus and that they outline the dusty torus around the central engine, as expected from current AGN models. From our first estimate of the fluxes in L and M, we derive a dust temperature of 750 K for the unresolved component.

1. Introduction

Active galactic nuclei (AGN) are extremely complex objects and so far, their geometry could be inferred only indirectly. Yet, geometrical parameters play a very important role in AGN models and their knowledge is therefore essential. Being the nearest and brightest Seyfert galaxy, NGC 1068 appears as the best candidate to approach directly the AGN geometry.

Advances in high resolution imaging from the ground, thanks to adaptive optic systems, now offer the opportunity to probe the inner structure of NGC 1068 in the near-infrared (1.25 to 5 μm). Such data may provide a hand on the dust/molecular torus location and contribute to probe the AGN unified theory.

The adaptive optic device available at ESO 3.6 m telescope (COME-ON+, later ADONIS) allows to image in K (2.2 μm), L (3.5 μm) and M (4.8 μm) bright objects such as the AGN in NGC 1068 with a spatial resolution approaching that achieved with the Hubble Space Telescope (HST) at visible and UV wavelengths.

In the current paper, we report on the distribution of the near-infrared emission at high angular resolution (resolution from 15 to 35 pc) from adaptive optic observations of the 2"$\times$ 2" (144 pc$\times$144 pc) nuclear region of NGC 1068, and on the relative positioning of the near-infrared and visible continuum peaks.

2. Set up for simultaneous observations in K band (2.2 μm) and I band (0.8 μm)

We used the ESO 3.60-meter telescope (La Silla, Chile) and the COME-ON+ adaptive optic system (Rigaut et al. 1991, Hubin et al. 1993) on the nights 28/29 October 1993 and 5/6 November 1993.

The adaptive optic correction was performed on the brightest spot of the nuclear region of NGC 1068 in the visible (Lynds et al., 1991). The wavefront sensor, an EBCCD, has a pixel size of 0.7" and takes into account the gravity center of the light within a 6" diameter circular entrance.

The imaging light-path arrives, after application of the adaptive optic correction, on the SHARP camera (System for High Angular Resolution infrared Pictures, Hofmann et al. 1992) at the f/45 Cassegrain focus, providing an image scale of 0.05"/pixel over a field of view of 12.8"$\times$ 12.8" (Fig. 1 top).

We also performed the particular experiment of adding, along the imaging light-path, a second dichroic foil to observe simultaneously in the visible (I band) with a CCD camera, and in the near-infrared (K band) with SHARP, in order to position and scale very accurately images in

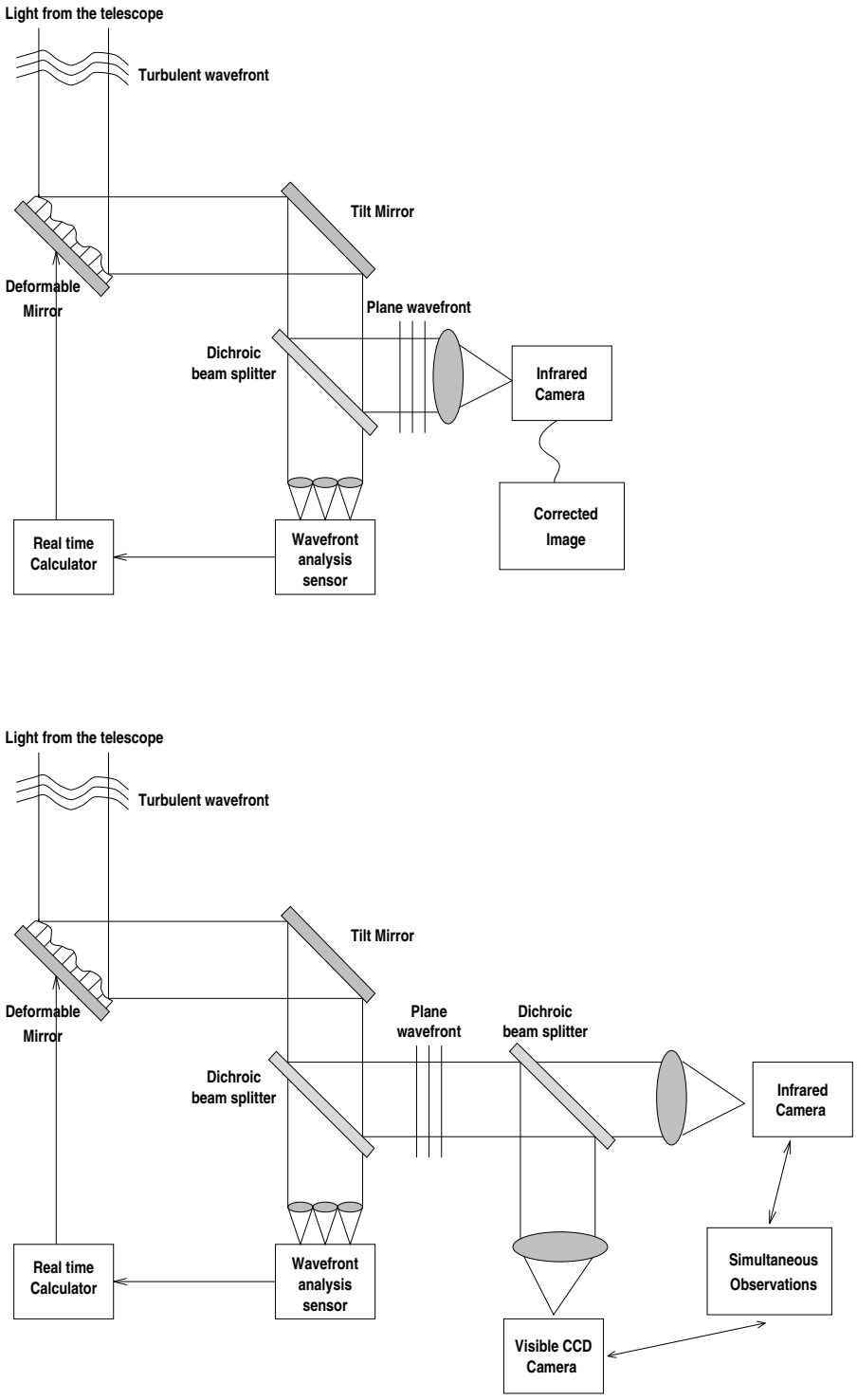

Figure 1. Top: Optical design of the COME ON+/ADONIS adaptive optic system. Bottom: Experimental setup for the simultaneous observation in K and I.

TABLE 1. Parameters of the K and I band COME-ON+ observations

Target	Band	Total integration time	FWHM N-S	FWHM E-W	comment
NGC 1068	K (2.2 μm)	44x(3 s)	0.45"	0.60"	
SAO 130075	K (2.2 μm)	11x(3 s)	0.45"	0.45"	reference star
NGC 1068	I (0.8 μm)	1x(120 s)	1.4"	1.3"	
SAO 130062	I (0.8 μm)	1x(5 s)	1.3"	1.3"	reference star

the two bands (Fig. 1 bottom). The image scale for the CCD camera was 0.034"/pixel, resulting in a field of view of 16.8"$\times$ 16.8".

During the two nights, the seeing was not much better than 1". Because of this and because the visible source in NGC 1068 used to close the adaptive optics loop has a magnitude of about 12, the efficiency of the adaptive optic correction was not optimal. Therefore, the final images obtained in K with SHARP were not diffraction limited and we reach only a resolution of 35 pc in K (FWHM=0.45" for the reference star).

Full details on data acquisition procedures are provided in Marco et al. (1997a). Standard infrared data reduction procedures were applied to each individual frame, for both the galaxy and the reference stars : mainly dead pixel removal, sky subtraction and flat fielding.

Flexure effects, differential refraction effects were all found to be quite small and are taken into account in the final errorbar.

We summarize in Table 1 the information about the data.

3. Results from the simultaneous observations in K and I

In order to locate with maximum accuracy the emission peaks in the near-infrared (K band) and in the visible (I band), we use the simultaneous images in these two bands.

We have first determined the pixel scaling between the two bands. We used two reference stars, observed three times simultaneously in the two bands. We computed their relative offsets in the infrared band, for which we know precisely the pixel scaling. Then we made the obvious assumption that the offsets for the stars are identical in the two bands, and deduced the pixel scale of the CCD camera. We also deduced from these measurements the orientation of the field of view for the CCD camera. The pixel sizes and the FWHM are different in the two bands : therefore, the positions

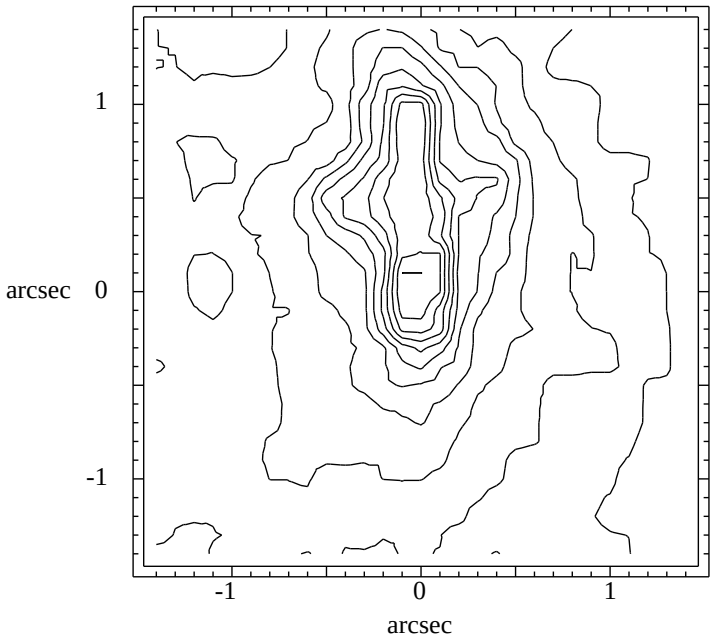

Figure 2. The 4.8 μm contour map of NGC 1068 with ADONIS, centered on the infrared peak. North is up, east to the left. The HST optical continuum peak (Lynds et al., 1991) would be located on this plot at $\approx$0.3" north of the infrared M peak.

of the maximum peaks corresponding to the galaxy and to the reference stars were estimated by fitting 2-dimensional Gaussian profiles, using the MIDAS package. Then, for each of the I and K band images, we determined the offsets between the maxima of the galaxy and of two reference stars, SAO 130062 and SAO 130080, without applying any deconvolution technique. We checked these results on several data sets (3 galaxy observations interlaced with 3 exposures on the 2 reference stars) always observed simultaneously in the two bands. These redundant measurements provide a 1σ error estimate of $\pm$0.03". Another more conservative estimate of the error bar is to consider that the gaussian fit to our data, given the signal to noise ratio, can be centered at 1/10 its FWHM. This provides a $\pm$0.05" error bar. We retain this value.

The K band maximum peak is found to be located 0.28 ± 0.05 " south, and 0.08 ± 0.05 " west from the I band continuum peak. This offset along the north-south direction is about half of the spatial resolution achieved on the deconvolved image. Given the signal-to-noise ratio of the data, we are confident that such an offset, although small, is significant (Marco et al., 1997a). In NGC 1068, the I band is essentially sensitive to continuum emission and the observed single peak in I is most probably the extension

at longer wavelengths of the bright continuum source observed by Lynds et al. (1991) at 5470 Å with the HST. Indeed, from a comparison between the locations of the reference star images in I and of the NGC 1068 peak in I, and given the fact that the position of either of these sources in the visible on the wavefront sensor is kept exactly at the same location, we conclude that there is no offset (larger than 0.05") between the I peak on NGC 1068 and the V continuum source within NGC 1068 on which the adaptive optic loop was closed. This is also confirmed by recent measurements from V and I band HST images obtained with the WFPC2 instrument, which demonstrate that, within 0.05", the peaks in these two bands occur at the same location (Z. Tsvetanov, private communication). Within the errorbars, the position we obtain for the K peak is consistent with that reported by Thatte et al. (1996, private communication, and this volume): 0.41 ± 0.10 " south, and 0.23 ± 0.10 " west of the HST optical continuum peak.

The K band image has been deconvolved using a Lucy-Richardson algorithm (40 iterations). The final FWHM is indicated in Table 1. The deconvolved image (Fig. 3) shows the presence of an extended emission within the central 100 pc around the hidden nucleus and an unresolved peak (at a resolution of 35 pc) which radiates more than 66% of the flux. The compact infrared source appears to be associated with dust heated directly by the central active nucleus, while the extended emission region may be related to additional local emitting processes (Marco et al., 1997a).

4. Observations and preliminary results in the L and M bands

In order to probe in a direct way the hot dust component in NGC 1068, (Glass, 1995), we have complemented the 2.2 μm results by data at longer wavelengths, namely in the L (3.5 μm) and M (4.8 μm) bands.

We have observed NGC 1068 with ADONIS, an upgraded version of the ESO adaptive optics system, equipped with the COMIC camera (Lacombe et al., 1997; Marco et al., 1997b). For most of the observing run, 1996 August 14 to 17, the seeing was superb, between 0.4" and 0.8". Again, the wavefront sensor was working with a pixel size of 0.7" and was taking into account the gravity center of the light within a 6" diameter circular aperture. Similarly to the previous K band observations, the adaptive optic correction was performed on the brightest V continuum peak in NGC 1068, as seen by the HST (Lynds et al., 1991).

The COMIC camera provides an image scale of 0.1"/pixel, and allows to probe a field-of-view of 12.8"×12.8". All the images collected during this run were diffraction-limited, providing resolutions of 0.24" (L band) and 0.33" (M band).

We alternated observations of the AGN and of a nearby reference star

in order to derive and monitor the point spread function (PSF). The optical peak in NGC 1068 (Lynds et al., 1991) on which the adaptive optics loop is closed constitutes the positional reference point in the field, and therefore corresponds also to the location of the PSF star center (the (0,0) point on Fig. 3). Flexure effects were found to be less than 1 pixel (<0.1") and differential atmospheric refraction effects were very small (<0.01"). We expect the final relative registration of the NGC 1068 images in L and M, with respect to the V peak, to be derived with a precision of 0.1".

We provide in Fig. 2 the M band image of the AGN without any deconvolution. It shows the existence of an unresolved core (size $\leq$23 pc) plus extended emission at 4.8 μm. In these preliminary results we also find that the M peak (the (0,0) point on Fig. 2) is displaced by $\approx$0.3 $\pm$ 0.1" to the south of the V peak in NGC 1068. Similar offsets are measured in the L band image of the AGN, which shows also an unresolved core (size $\leq$15 pc) and an extended emission region. Complete results will be found in Marco et al. (1997c).

5. Conclusion

We provide on Fig. 3 the final comparative registration of the AGN maps, from UV to infrared, adding the new K (2.2 μm), L (3.5 μm) and M (4.8 μm) band results. The relative positioning of the radio components and maser emission are discussed elsewhere in this volume.

With respect to the HST optical continuum peak (Lynds et al., 1991), the near-infrared peak (found to be at the same position in K, L and M bands) coincide with the center of polarization in the UV (Capetti et al., this volume) and is enclosed within the errorbox of the 12.4 μm emission (Braatz et al., 1993).

We conclude that the infrared peaks are directly related with the hidden nucleus, and outline the dusty torus around the central engine, as expected from current AGN models (Pier and Krolik, 1992; Efstathiou et al., 1995). From our first estimate of the fluxes in L and M, we derive a dust temperature of 750 K for the unresolved component.

References

Braatz, J.A., Wilson, A.S., Gezari, et al., 1993, ApJ, 409, L5
Capetti, A., Axon, D.J., Macchetto, F., Sparks, W.B., Boksenberg, A., 1995, ApJ, 452, L87
Efstathiou, A., Rowan-Robinson, M., 1995, M.N.R.A.S., 273, 649
Evans, I.N., Ford, H.C., Kinney, A.L., et al., 1991, ApJ, 369, L27
Glass, I.S., 1995, M.N.R.A.S., 276, L65
Hofmann R., Blietz M., Duhoux P., et al., 1992, In: Ulrich M.-H. (ed), Progress in Telescope and Instrumentation Technologies, ESO, Garching, 687
Hubin, N., Rousset, G., Beuzit, J.L., et al., 1993, Messenger 71, 50

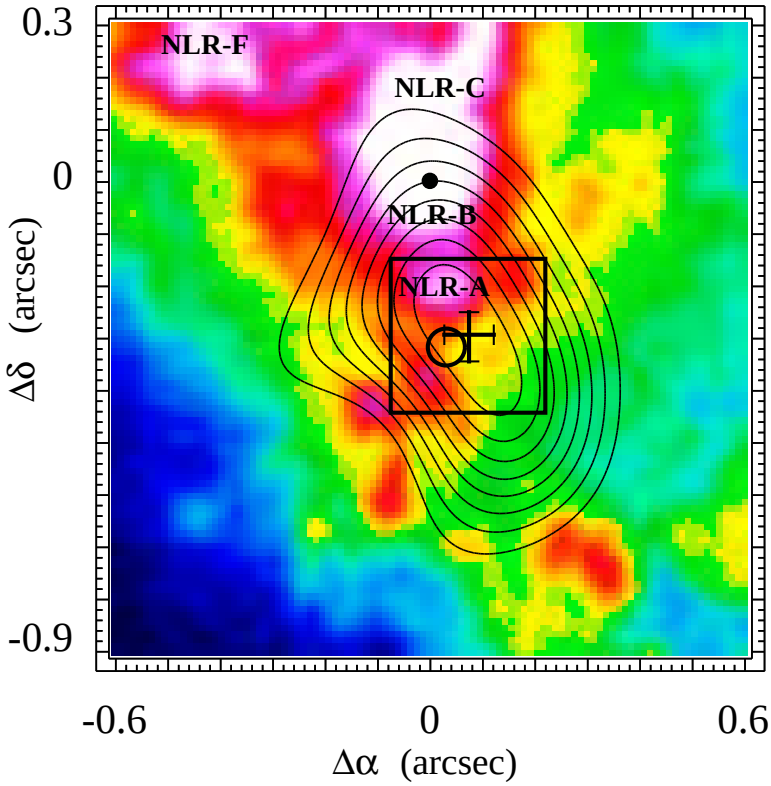

Figure 3. Contour map of NGC 1068 in the K band (linearly scaled from 10% to 100% of the peak intensity), overlaid on an image from the HST in the [O III] line (Macchetto et al., 1994), centered on the HST optical continuum peak. We show the [O III] line NLR-clouds as identified by Evans et al. (1991). North is up, east to the left.
Symbols are :
dot : the HST optical continuum peak (Lynds et al., 1991) ;
box (size indicates errorbar) : the 12.4 μm peak positioned by Braatz et al. (1993) ;
cross (size indicates errorbar) : near-infrared peaks location (same for K, L and M bands), from Marco et al. 1997a,b ;
circle (size indicates errorbar) : the symmetry center of the UV/optical polarization (Capetti et al., 1995).

Lacombe, F., Marco, O., Geoffray, H., et al., 1997
Lynds, R., Faber, S.M., Groth, E.J., et al., 1991, ApJ, 369, L31
Macchetto, F., Capetti, A., Sparks, W.B., 1994, ApJ, 435, L15
Marco, O., Alloin, D., Beuzit, J.L., et al., 1997a, A&A, 320, 399
Marco, O., Lacombe, F., Geoffray, H., et al., 1997b
Marco, O., Alloin, D., Lacombe, F., Veran, J.P., 1997c, A&A, in preparation
Pier, E.A., Krolik, J.H., 1992, ApJ, 401, 99
Rigaut, F., Rousset, G., Kern, P., et al., 1991, A&A, 250, 280